Available online at www.sciencedirect.com
SCIENCE DIRECT®
Pergamon
Cement and Concrete Research 33 (2003) 1449–1456
CEMENT AND CONCRETE RESEARCH

Surface alteration of dolomite in dedolomitization reaction in alkaline media

E. García*, P. Alfonso, E. Tauler, S. Galí

Departament de Cristal-lografia, Mineralogia i Dipòsits Minerals, Universitat de Barcelona, C/Martí i Franquès s/n, 08028 Barcelona, Catalonia, Spain

Received 6 December 2002; accepted 28 February 2003

Abstract

The phases precipitated on the dolomite surface and the influence of alkalis on the properties of this surface were characterized. Experiments consisted of the immersion of single crystals of dolomite in saturated portlandite solutions with different alkalinity, temperature, and silica content.

Most calcite forms in the solution as {104} rhombohedra. Brucite crystallizes as platelets, piles of platelets, sponge-like and {001} truncated ditrigonal pyramids attached to the dolomite surface. The morphology of brucite crystals depends on the pH of the solution. Apparent dissolution rate constants for dolomite at 75 °C are one order of magnitude higher than at room temperature.

Initially, calcite grows on the dolomite surface with the same structural orientation {104}. In a second stage, when calcite has reached equilibrium with the solution, the new-formed {104} calcite surface starts playing an important role on the precipitation of brucite, while calcite continues crystallizing in the bulk solution. The calcite surface, negatively charged, can adsorb specifically metal cations. Mg^{2+}, liberated by the dissolution of dolomite, would move attached to the surface, until they are trapped on these negatively charged surfaces, while OH^- supplied by the alkaline solution favors the nucleation and growth of brucite. The attachment of Mg^{2+} to the surface controls the place where brucite grows.

Keywords: Kinetics; Alkali–aggregate reaction; Dolomite–portlandite

1. Introduction

The reactions that take place between carbonate rock and portland cement paste have drawn the attention of several researchers [1,2]. In particular, dolomite–alkali reactions have been studied by many authors on account of the claim of its potential expansive character [2–4].

Dedolomitization of dolomite aggregate in mortars and concretes takes place in different manners, depending on the composition of the chemical system. For alkaline media resembling those encountered in portland mortars, several reactions may be observed, but only one seems to be relevant, as long as portlandite is present in the system [5,6]:

$$CaMg(CO_3)_2 + Ca(OH)_2 = 2CaCO_3 + Mg(OH)_2$$

In this reaction, the limiting step has been found to be the dissolution of dolomite.

Several points are relevant regarding this reaction in mortars. Since the calcite–brucite pair is more stable, the reaction should progress until completion. However, in a series of experiments [5,6], it has been found that this result, as a rule, is only achieved at high temperature (75 °C), where the alkali increases the overall rate of the process. At room temperature, we can distinguish two stages in the whole reaction. In the first one, reaction proceeds with a higher rate, while in a second stage, the reaction slows down abruptly before the complete dissolution of dolomite. At room temperature, the effect of the addition of alkali is contrary to that observed at 75 °C, reducing the overall dissolution rate constant of dolomite. In the previous works cited above, two mechanisms for the reduction of dissolution rates were suggested. One preliminary experiment showed that calcite and possibly brucite precipitate on dolomite, reducing the area being dissolved. Another possibility taken into account was the alteration of the dolomite surface properties by the adsorption of the charged chemical species in solution (mainly OH^-, H^+, Ca^{2+}, and CO_3^{2-}), whose concentration depends mainly on pH and temperature. These species may react with the dolomite surface

* Corresponding author. Tel.: +34-93-402-1354; fax: +34-93-402-1340.
E-mail address: engarcia@natura.geo.ub.es (E. García).

0008-8846/03/$ – see front matter © 2003 Elsevier Ltd. All rights reserved.
doi:10.1016/S0008-8846(03)00096-6

creating surface complexes and modifying the surface charge. All these factors are liable to modify the dissolution rates of carbonates and other minerals [7]. The reactions described in Refs. [5] and [6], based on a dispersion of powders, did not permit a detailed observation of the modification of the surface of dolomite crystals. This is the reason for undertaking a new series of experiments based on the immersion in different solutions of large areas (100 mm^2) of exfoliated dolomite crystals. The size of these samples permits us to use comfortably the methods of physical characterization of phases like scanning electron microscopy (SEM), X-ray diffraction (XRD), and X-ray texture analyses. The solutions used imitate the reported pore solutions in portland cement paste [8].

In summary, the purpose of the present work is to characterize the phases precipitated on the dolomite surface, the influence of alkalis on the properties of the surface affecting the dissolution rates of dolomite, and the overall influence of these factors on the durability of concretes and mortars made of dolomitic aggregates.

2. Experimental procedure

The basic experiment consists of the immersion of a single crystal of dolomite in a saturated portlandite solution. Four initial water solutions were used: (1) pure water; (2) 0.1 M NaOH solution; (3) 0.1 M KOH solution; (4) 0.6 M KOH equivalent solution (0.45 M KOH+ 0.15 M NaOH).

Gem-quality crystals of dolomite with approximate dimensions 6×6×2 mm were used. They exhibited perfect rhombohedral exfoliation {104}. Electron microprobe analyses of the bulk solid and powder diffraction confirmed the purity of the material. "Alfa" commercial $Ca(OH)_2$ powders from Johnson and Matthey were used. The BET surface, measured using a N_2 adsorption isotherm, was 16.5 $m^2\ g^{-1}$. The starting water solutions (8 ml), the portlandite powder (in excess), and the dolomite crystals were introduced in Teflon bottles provided with a cap to avoid atmospheric carbonation. Crystals were suspended in the solution by means of a thin platinum wire. The content was stirred every 30 min.

For each composition, two different runs were performed at 25 and 75 °C. The duration of the experiments was 60 and 15 days, respectively. After this period of time, dolomite crystals were removed from the water solution and washed with methanol. The solid particles dispersed in the solutions were filtered through Millipore filters with 0.22 μm pore diameter. Both dolomite crystals and powders were carefully weighed.

Characterization of the filtered solution included pH measurement with a high-alkalinity-suitable electrode and cation analyses by ICP-AES (Perkin Elmer Elan 6000). Quantitative analyses for the crystalline solids retained by the filters were achieved by full diffraction profile-matching method (quantitative Rietveld analysis). Since the {104} dolomite surfaces were dissolved and/or covered by the products of the reaction, the structure of the resulting surfaces were carefully characterized using different techniques. The average composition and texture of deposited crystals were investigated by means of conventional powder diffraction, including θ/2θ and ω scans, and the dolomite single crystal acts as a substrate. In several samples, X-ray texture analyses were performed as well. For a more detailed vision of the structure of these reaction layers, the surfaces were observed by SEM. Atomic force microscopy (AFM) gave useful details on the mechanism of growth of brucite crystals on {104} dolomite surface.

Table 1
Mineralogy and texture of the solids precipitated on the dolomite surface and in the solution and chemical parameters for the different experiments at room temperature

Solution	Pure water		0.1 M NaOH		0.1 M KOH		0.6 M KOH eq.	
Solids crystallizing on dolomite surface	fibrous brucite small crystals of calcite		layer of brucite small crystals of calcite		layer of brucite calcite {104} parallel to substrate		layer of massive brucite calcite {104} parallel to substrate	
Solids recovered in filter (wt.%)	calcite	91.5	calcite	55.5	calcite	60.3	calcite	67.4
	dolomite	8.5	dolomite	1.0	dolomite	0.2	dolomite	1.8
	huntite	traces	portlandite	43.5	portlandite	39.5	portlandite	30.8
Saturation index at the end of the experiment	dolomite	−1.55	dolomite	−1.24	dolomite	−1.07	dolomite	−0.84
	brucite	3.30	brucite	4.10	brucite	4.50	brucite	4.63
	portlandite	−0.23	portlandite	0.26	portlandite	0.50	portlandite	0.38
pH		12.31		12.89		13.05		13.59
Apparent dissolution rate constant (mol $m^{-2}\ s^{-1}$)		5.7×10^{-8}		3.0×10^{-8}		3.5×10^{-8}		1.1×10^{-7}

3. Results

3.1. Experiments at 25 °C

Main results for experiments performed at room temperature are summarized in Table 1. A selection of SEM images of dolomite surfaces are given in Fig. 1.

As a rule, most calcite nucleates and grows in the solution, forming small {104} rhombohedra. Only a small fraction of total calcite can be observed on the dolomite surface, as rhombohedra orientated parallel to {104} faces of dolomite, forming an epitactic discontinuous layer. This is clearer for experiments 0.1 M KOH and 0.6 M KOH equivalent.

Brucite is not observed in recovered powders. It crystallizes on the dolomite surface or near it. Crystals, however, are not firmly attached to the surface and can be lost easily when these surfaces are washed with methanol. The morphology of brucite crystals apparently depends on the pH of the solution: for pH<12.3, it crystallizes in the fibrous variety named nemalite (Fig. 1a), while for pH>13 brucite forms a crust on dolomite surface with dominant orientation {001} and {101} (Fig. 1b). Other minor phases suggested by diffraction are potassium and/or sodium carbonates.

In all experiments, dissolution areas of dolomite can be observed (Fig. 1c). These areas are completely free from any deposition of calcite or brucite.

The saturation indexes for dolomite, brucite, and portlandite are calculated on the basis of the analytical results, under the condition that calcite is always in equilibrium. This assumption appears a realistic one, since induction periods for nucleation of calcite are very low compared with the duration of the experiment [9]. Chemical equilibrium calculations were performed using the EQ3NR computer program [10]. The apparent constant rates for the dissolution of dolomite are calculated on the basis of the initial area of the crystal and considering that the exposed surfaces are ideally flat. These values are given only for comparison purposes and should not be taken as "real" values. The assumption of flat perfect surfaces is not realistic, since dissolution corrodes the crystal and greatly increases the dissolving surface. On the other hand, the area covered by precipitated calcite and brucite can hardly be estimated.

3.2. Experiments at 75 °C

Results for experiments at 75 °C are summarized in Table 2. SEM images and XRD of dolomite surfaces are shown in Figs. 2 and 3, respectively. Figs. 4 and 5 show pole figures obtained for calcite and brucite on {104} dolomite surface for sample 0.6 M KOH equivalent.

Most calcite crystallizes in the solution. The fraction crystallizing on dolomite surfaces shows a single 104 peak in the diffractogram orientated parallel to {104} faces of dolomite, forming an epitaxial layer more continuous and thicker than in the experiments at room temperature (Fig. 2a).

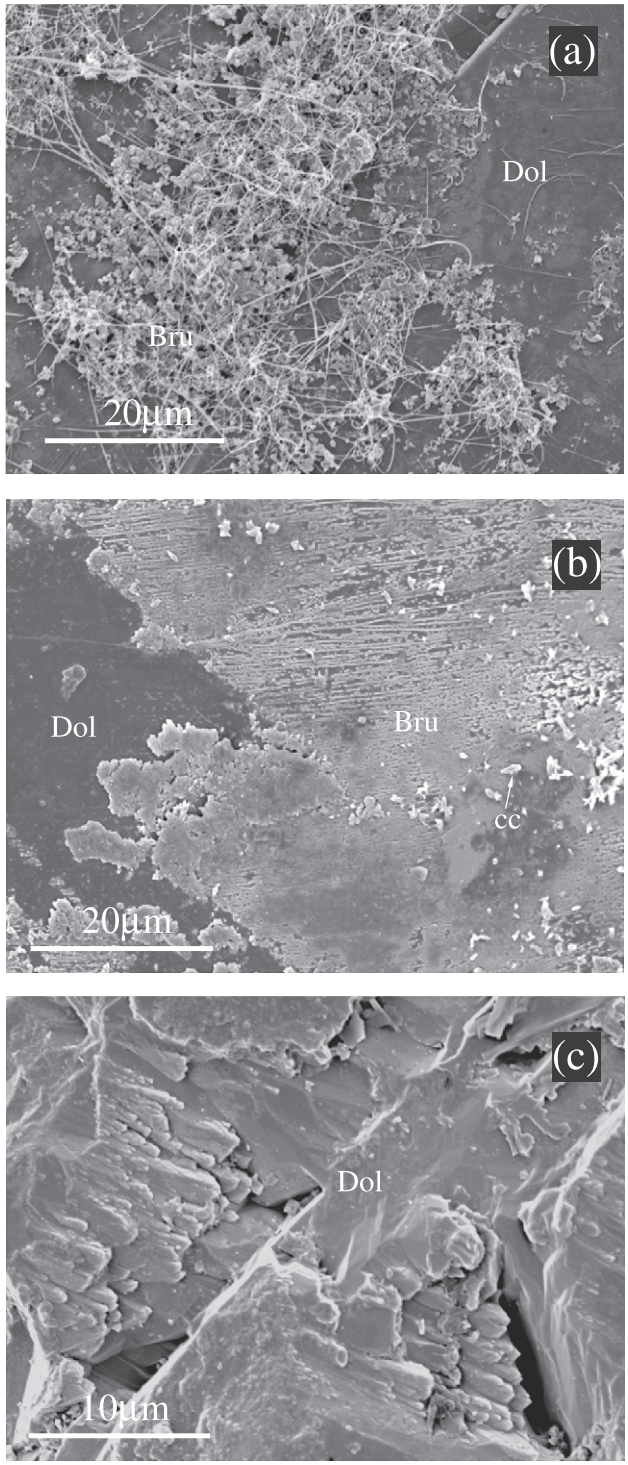

Fig. 1. Selection of SEM images of dolomite surface in experiments at 25 °C. (a) Fibrous variety of brucite (nemalite). (b) Crust of brucite on dolomite surface with dominant orientation {001} and {101}. (c) Dissolution areas of dolomite.

The relative intensity of X-ray spectrum between 104 peaks of calcite and dolomite allows the estimation of the thickness of the epitaxy. For example, in case of experiment 0.1 M KOH, it is less than 1 μm in thickness (Fig. 4).

Table 2
Mineralogy and texture of the solids precipitated on the dolomite surface and in the solution and chemical parameters for the different experiments at 75 °C

Solution	Pure water		0.1 M NaOH		0.1 M KOH		0.6 M KOH eq.	
Solids crystallizing on dolomite surface	sponge like and massive brucite few calcite		layer of brucite calcite {104} parallel to substrate		layer of massive and sponge-like brucite calcite {104} parallel to substrate		{001}+{211}+{12l} oriented brucite massive {104} calcite	
Solids recovered in filter (wt.%)	calcite	99.0	calcite	76.5	calcite	66.1	calcite	85.7
	dolomite	1.0	dolomite	0.8	dolomite	0.0	dolomite	3.5
			portlandite	19.2	portlandite	29.7	portlandite	10.9
			brucite	3.5	brucite	4.2	brucite	0.0
Saturation index at the end of the experiment	dolomite	−0.61	dolomite	−0.47	dolomite	−0.81	dolomite	−0.18
	brucite	3.99	brucite	4.96	brucite	5.05	brucite	5.96
	portlandite	0.19	portlandite	1.00	portlandite	1.44	portlandite	1.75
pH		11.07		11.84		12.00		12.57
Apparent dissolution rate constant (mol m^{-2} s^{-1})		5.5×10^{-7}		5.5×10^{-7}		1.2×10^{-7}		6.0×10^{-7}
Activation energy (kJ mol^{-1})		39.15		50.20		21.34		29.28

Brucite is only observed in very small amounts in recovered powders. Most brucite is then formed on the dolomite surface. At 75 °C, the fibrous morphology is not observed. Instead, platelets, piles of platelets (Fig. 2b), sponge-like (Fig. 2c) and {001} truncated ditrigonal pyramids attached to the dolomite surface (Fig. 2d) were found. Evidence of spiral growth of brucite in sample 0.6 M KOH equivalent is given by the AFM image of Fig. 6. These brucite crystals make a first layer covering large areas of the dolomite surface, until a new generation of smaller crystals grows in disorder with a pseudodomiant {101} orientation. Fig. 5a and b shows the 001 and 101 pole figures of brucite for sample 0.6 M KOH equivalent. All dolomite crystals observed by SEM display dissolution areas, sometimes with a columnar morphology.

Dolomite is always undersaturated at the end of the experiment. Portlandite is slightly supersaturated, while brucite is always highly supersaturated. Apparent dissolu-

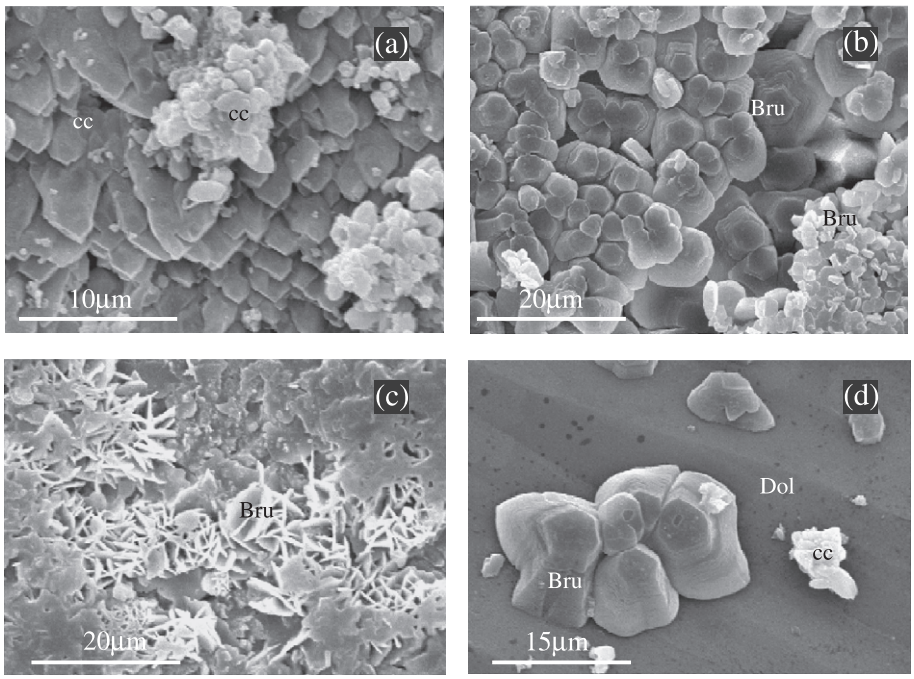

Fig. 2. Selection of SEM images of dolomite surface in experiments at 75 °C. (a) Rhombohedral epitaxial crystals of calcite on dolomite surface. (b) Platelets and piles of platelets of brucite covering the dolomite crystal. (c) Sponge-like texture of brucite covering the dolomite crystal. (d) Truncated ditrigonal pyramids of brucite attached to the dolomite surface.

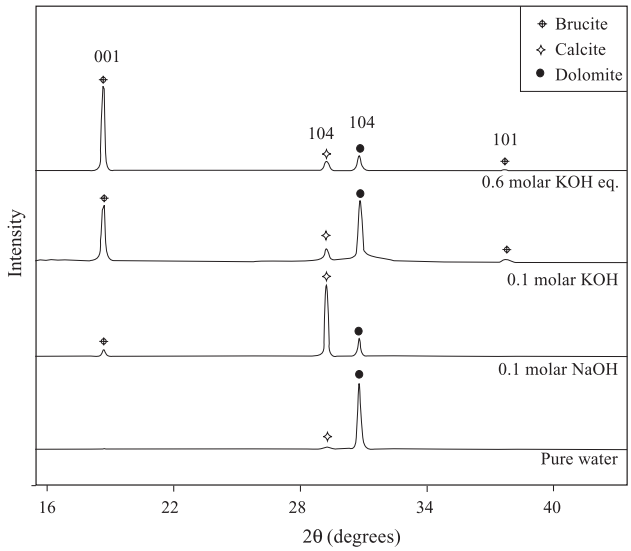

Fig. 3. X-ray diffraction patterns of dolomite surface in experiments at 75 °C.

tion rate constants for dolomite are systematically one order of magnitude higher than the values obtained at room temperature.

4. Discussion

Nucleation and growth of calcite and brucite requires the dissolution of dolomite, which affords CO_3^{2-}, Ca^{2+}, and Mg^{2+} ions. As clearly observed by SEM, there are areas of the dolomite surface that dissolve, while calcite, brucite, or both minerals cover other areas that will not dissolve. Experiments on dissolution of solids show that at the molecular level, the dissolution process is roughly the opposite of that during growth. Higher concentration of defects, as subgrain boundaries and dislocations, may favor a faster dissolution of the crystal in these areas. It appears then that under subsaturation conditions, once one area of the crystal starts to dissolve, its roughness increases, which in turn accelerates the dissolution. In addition, the stirring conditions and the geometry of the experiment may have created flow patterns favoring the

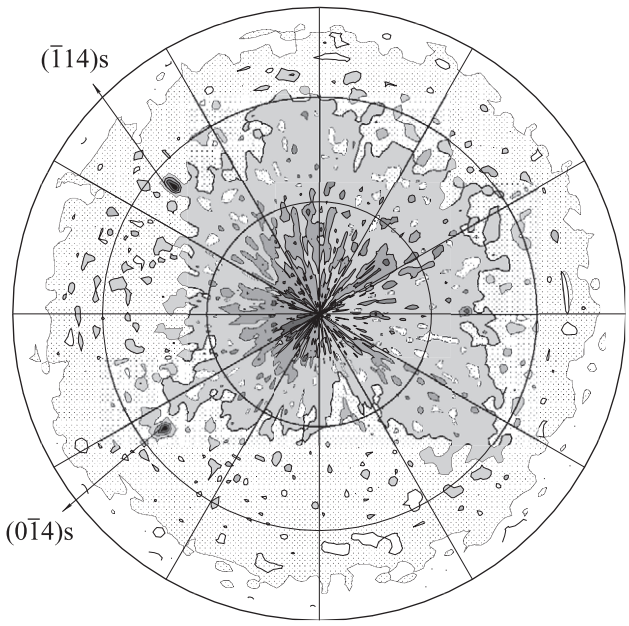

Fig. 4. (104) Pole figure obtained for calcite grown on {104} dolomite surface, for sample 0.6 M KOH equivalent.

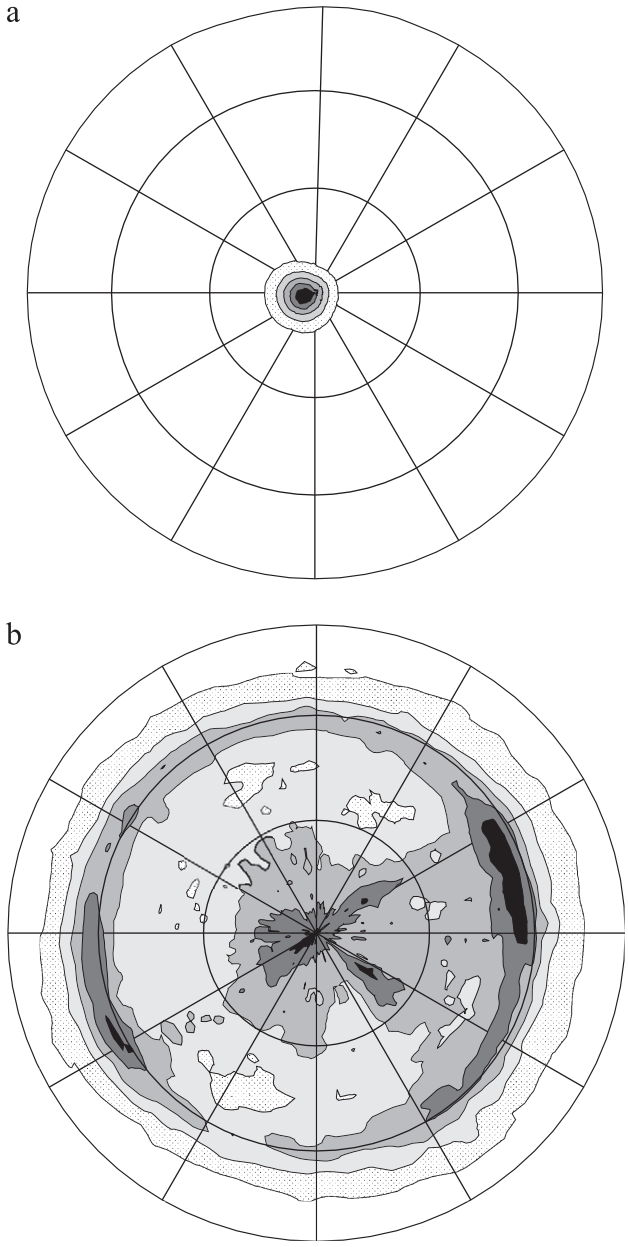

Fig. 5. Pole figures obtained for brucite on {104} dolomite surface for sample 0.6 M KOH equivalent; (a) (001) pole figure and (b) (101) pole figure.

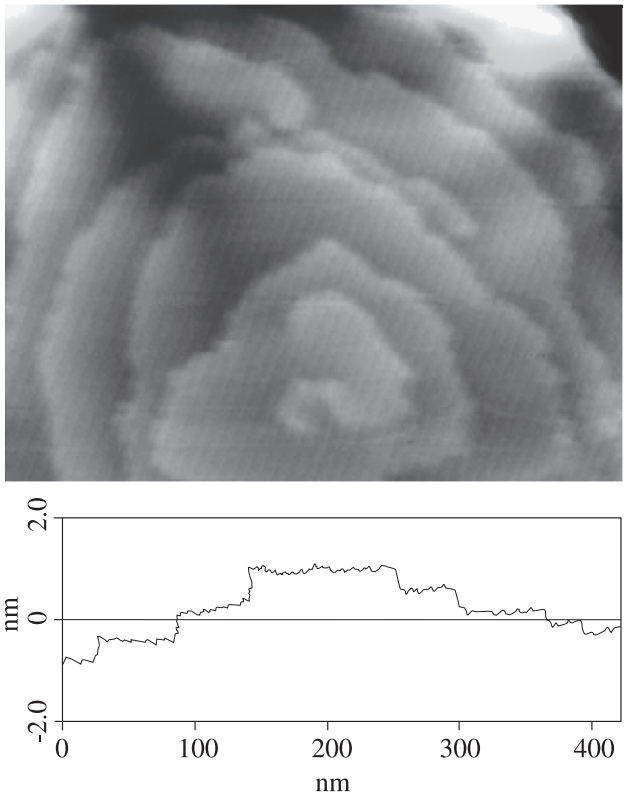

Fig. 6. Spiral growth of brucite in sample 0.6 M KOH equivalent shown by AFM image. Height profile along the white line drawn in the image. The height of the steps is 0.4 nm.

dissolution of certain parts of the crystal. Fig. 1c shows a columnar dissolution that seems able to detach small particles from the dolomite crystal. These particles have been recovered after filtration and always represent a small amount of recovered powders. We discard completely the possibility that these dolomite particles could nucleate and grow from the solution, given that dolomite is always undersaturated.

The dissolution of dolomite affords two CO_3^{2-} anions for each Ca^{2+} cation. According to the stoichiometry of the dedolomitization reaction, nucleation and growth of calcite requires the contribution of another source of Ca, which is provided by portlandite. This may explain why most calcite nucleates and grows in the bulk of the solution. Calcite particles recovered by filtration have a pronounced monodispersed character (Fig. 7), which requires that only one burst of nuclei occurs when a critical supersaturation is reached. Such conditions can be found when one of the precipitating components is released into the solution under a kinetic control, and it is supposed that this role could be played by the slow dissolution of dolomite.

In addition, given the structural affinity between calcite and dolomite, calcite grows as well on the dolomite surface with the same structural orientation {104}. This is demonstrated by diffraction: conventional powder diffraction on dolomite surface displays only the peak 104 for calcite, the corresponding rocking curve is narrow (1.6° 2θ) and 104 pole figure gives a single peak (Fig. 4). Then, it could be inferred that the first calcite to precipitate forms a true epitaxy on dolomite. The epitaxial layer is very thin, but may effectively reduce the dissolution surface of dolomite. At 25 °C in pure water solution, the epitaxial layer has not been observed. The growth of the initial layer of calcite is interrupted abruptly, and brucite will be the next phase to be deposited on this modified surface. The structure and bonding environments of the surfaces of dolomite and calcite are likely to play a determinant role in the succession of phases appearing on the {104} dolomite surface.

Given the structural affinity between both carbonates and the possibility of partial solid solution between them, it can be accepted that calcite precipitates on several areas of dolomite before its pristine exfoliation surface be modified by dissolution (etch pits) or adsorption of chemical species in solution. The calcite supersaturation needed for such homogeneous bidimensional nucleation should be very low. In a second stage, when calcite has reached equilibrium with the solution, the new-formed {104} calcite surface starts playing an important role on the precipitation of brucite, while calcite continues to nucleate and grow in the bulk solution. For solutions with pH above 12.5 at room temperature (or pH>11 at 75 °C), brucite appears to block the growth of epitaxial calcite.

Most minerals, tend to acquire a negative surface charge at high pH. On the contrary, at low pH, the surface charge becomes positive. In general, there is a pH value, pH_{pzc}, where the surface charge is zero. For mineral carbonates, things are a little more complex, since pH is not the only determining parameter of the point of zero charge [11]. Other potential determining species affecting calcite surface charge are Ca^{2+}, $CaOH^{+}$, HCO_3^{-}, CO_3^{2-}, and so on, depending on partial pressure of CO_2, ionic strength, and other factors [12]. In our solutions, isolated from atmospheric carbon dioxide, the main potential determining

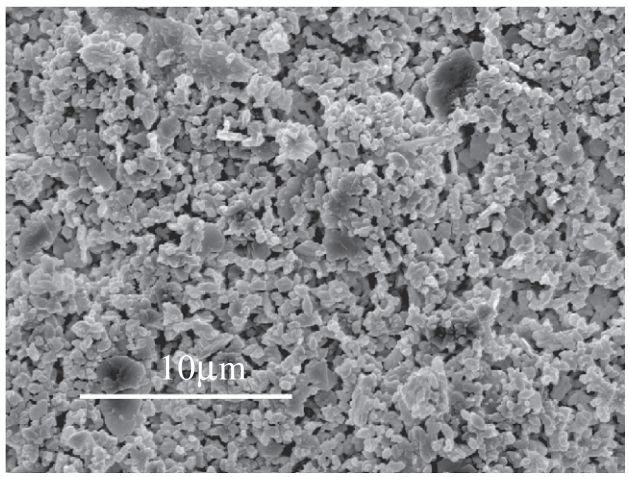

Fig. 7. SEM image of the solids retained after filtration. Calcite particles show a monodispersed character.

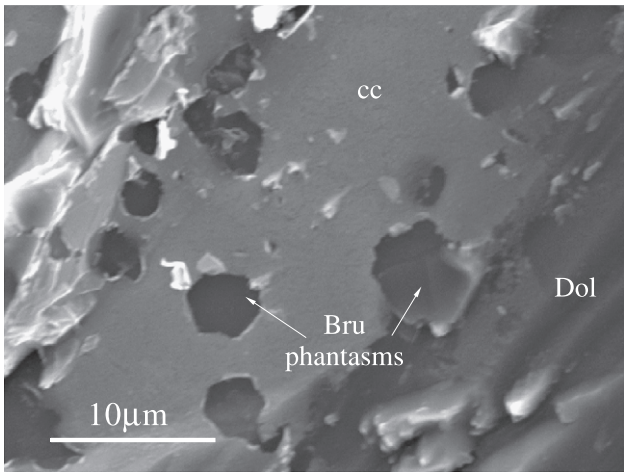

Fig. 8. Simultaneous growth of calcite and brucite on dolomite. The SEM image shows the negative crystals left by brucite crystals on the calcite layer.

species in solution are supposed to be OH^- and Ca^{2+}. The concentration of OH^- is between one to three orders of magnitude greater than that of Ca^{2+}. The calcite surface is supposed to be negatively charged through the following surface reactions [12]:

(a) $S{\cdot}Ca^+ + OH^- \rightarrow S{\cdot}CaOH^0$
(b) $S{\cdot}HCO_3 + OH^- \rightarrow S{\cdot}CO_3^- + H_2O$

where S stands for "surface." It has been observed that under these conditions, calcite surfaces can adsorb specifically metal cations [12,13]. Magnesium cation, which is liberated at a low rate by the dissolution of dolomite would move attached to the surface (surface diffusion), until it is trapped on these negative-charged surfaces, while OH^- supplied by the alkaline solution favors the nucleation and growth of the first brucite layer. Since only very few, if any, brucite has been observed in filtered suspension, it is concluded that the stirring is not sufficient to drive significant amount of Mg^{2+} to the bulk solution. The attachment of magnesium ions to the surface is then controlling the place where brucite grows. At 75 °C, for solution 0.6 M KOH, when the undersaturation of dolomite is lower, brucite nucleates directly on the dolomite surface, probably through the same mechanism described above. In these conditions, both calcite and brucite grow simultaneously on dolomite. Fig. 8 show the traces left by brucite crystals on the calcite layer, when they were detached from the dolomite surface.

The saturation index of brucite is always high and increases with pH and temperature. Different morphologies of brucite may indicate different conditions of growth influenced by the conditions of the solution and the changing properties of the calcite and dolomite surfaces as the process goes on. For instance, fibrous brucite is only observed at low pH and temperature, and apparently, it does not impede the dissolution of dolomite. This could explain the higher rates of dissolution encountered when alkali is not added to solution [5]. Multinucleated "sponge-like" equidimensional aggregates of brucite are usually observed not directly on dolomite, but as a second layer, when the supply of magnesium is reduced. Finally, crystals that have nucleated directly on the dolomite surface displaying a neat trigonal morphology have grown by spiral growth (BCF mechanism, Ref. [14]). This morphology produces a compact, well-oriented {001} layer parallel to {104} dolomite face which gives a single centered peak in the pole figure (Fig. 5a).

The apparent dissolution rate constants for dolomite, k_{dol} listed in Table 1, can be compared with those given in the literature [15,16], 2.2×10^{-8} mol m^{-2} s^{-1}. Figures obtained in the present work are not significantly different from the above value. The main discrepancies may arise from the estimation of the effective dissolving surface. Values of k_{dol} at 75 °C allow the calculation of the energies of activation for the dissolution of dolomite in different solutions (Table 2). The values obtained from the experiments are slightly higher than those given in the literature [17], but are similar to values obtained for us in previous experiments [5,6].

5. Conclusions

In the conditions of the experiments, dolomite is always undersaturated, but there are areas where dolomite dissolves and other areas that are covered by calcite and/or brucite.

Part of calcite precipitates epitactically on dolomite surfaces, on account of the similarity between both structures. Calcite nucleates and grows in the bulk solution.

The epitactic growth of calcite reduces dolomite and enlarges calcite surfaces, so that subsequent calcite will grow on new calcite surfaces, while dolomite continues dissolving at a lower rate.

Brucite morphology is dependent on pH and temperature. At low pH and room temperature, brucite forms the fibrous variety nemalite. At high pH and temperature, brucite nucleates over dolomite and/or calcite. Mobility of Mg^{2+} is very reduced, so that brucite is never encountered in the bulk solution.

Acknowledgements

The ICP-AES analyses were performed at the Serveis Científico-Tècnics (SCT) de la Universitat de Barcelona. X-ray diffraction analyses were performed at the X-ray unit at the SCT (X. Alcobé). E. Garcia acknowledges the receipt of an FPU fellowship from the Spanish Ministerio de Educación y Cultura. This research was sponsored by the CICYT Spanish research project MAT2001-3345 and contract RED99-57.

References

[1] P.J.M. Monteiro, P.K. Metha, Interaction between carbonate rock and cement paste, Cem. Concr. Res. 16 (2) (1986) 127–134.

[2] E.G. Swenson, J. Gillott, Alkali reactivity of dolomitic limestone aggregate, Mag. Concr. Res. 19 (59) (1967) 95–104.

[3] J.E. Gillot, E.G. Swenson, Mechanism of the alkali-carbonate rock reaction, Q. J. Eng. Geol. 2 (1969) 7–23.

[4] M.S. Tang, Z. Liu, S. Han, Mechanism of alkali-carbonate reaction, Proc. 7th Intl. Conf. on Alkali–Aggregate Reaction, Noyes Publications, Otawa, Canada, 1986, pp. 275–279.

[5] S. Galí, C. Ayora, P. Alfonso, E. Tauler, M. Labrador, Kinetics of dolomite–portlandite reaction. Application to Portland cement concrete, Cem. Concr. Res. 31 (6) (2001) 933–939.

[6] E. García, P. Alfonso, M. Labrador, S. Galí, Dedolomitization in different alkaline media: application to Portland cement paste, Cem. Concr. Res. (2003) (in press).

[7] A.C. Lasaga, Kinetic Theory in the Earth Sciences, Princeton Univ. Press, New Jersey (1998) 121–129.

[8] K. Andersson, B. Allard, M. Bengtsson, B. Magnusson, Chemical composition of cement pore solution, Cem. Concr. Res. 19 (3) (1989) 327–332.

[9] O. Söhnel, J.W. Mullin, Precipitation of calcium carbonate, J. Crystal Growth 60 (1982) 239–250.

[10] T.J. Wolery, EQ3NR, a computer program for geochemical aqueous speciation-solubility calculation: theoretical manual, user's guide and related documentation (Version 7.0), Publ. UCRL-MA-110662 Pt III, Lawrence Livermore Lab, Livermore, CA, USA, 1992.

[11] L. Charlet, P. Wersin, W. Stumm, Surface charge of $MnCO_3$ and $FeCO_3$, Geochim. Cosmochim. Acta 54 (1990) 2329–2336.

[12] W. Stumm, Chemistry of the Solid–Water Interface, Wiley-Interscience, Wiley, New York, 1992.

[13] J.M. Zachara, J.A. Kittrick, J.B. Harsh, The mechanism of Zn^{2+} adsorption on calcite, Geochim. Cosmochim. Acta 52 (1988) 2281–2291.

[14] W.K. Burton, N. Cabrera, F.C. Frank, The growth of crystals and the equilibrium structure of their surfaces, Phil. Trans. R. Soc. A 243 (1951) 299–358.

[15] W.P. Inskeep, P.R. Bloom, An evaluation of rate equations of calcite precipitation kinetics at pCO_2 less than 0.01 atm and pH greater than 8, Geochim. Cosmochim. Acta 49 (1985) 2165–2180.

[16] E. Busenberg, L.N. Plummer, The kinetics of dissolution of dolomite in CO_2–H_2O systems at 1.5 to 65 °C and 0 1 atm p_{CO_2}, Am. J. Sci. 282 (1982) 45–78.

[17] L. Chou, R.M. Garrels, R. Wollast, Comparative study of the kinetics and mechanism of dissolution of carbonate minerals, Chem. Geol. 78 (1989) 269–282.